Received: 9 June 2019 | Revised: 7 August 2019 | Accepted: 8 August 2019

DOI: 10.1002/er.4846

RESEARCH ARTICLE

WILEY INTERNATIONAL JOURNAL OF ENERGY RESEARCH

Implementation of repowering optimization for an existing photovoltaic-pumped hydro storage hybrid system: A case study in Sichuan, China

Xiao Xu[1] | Weihao Hu[1] | Di Cao[1] | Wen Liu[2] | Zhe Chen[3] | Henrik Lund[4]

[1]School of Mechanical and Electrical Engineering, University of Electronic Science and Technology of China, Chengdu, China

[2]Energy & Resources, Copernicus Institute of Sustainable Development, Faculty of Geosciences, Utrecht University, Utrecht, The Netherlands

[3]Department of Energy Technology, Aalborg University, Aalborg, Denmark

[4]Department of Planning, Aalborg University, Aalborg, Denmark

Correspondence
Weihao Hu, School of Mechanical and Electrical Engineering, University of Electronic Science and Technology of China, Chengdu, China.
Email: whu@uestc.edu.cn

Funding information
National Key Research and Development Program of China, Grant/Award Number: 2018YFB0905200

Summary

For a remote area or an isolated island, where the grid has not extended, a standalone hybrid energy system can provide cheap and adequate power for local users. However, with the development of society, the load demand will increase and the original system cannot completely meet the load demand. This situation occurs in Xiaojin, Sichuan, China. The existing photovoltaic-pumped hydro storage (PV-PHS) hybrid system in this area as the original system cannot completely meet the load requirements at present. The term "repowering" aims to maximize the reliability of power supply and the utilization of the PV-PHS hybrid energy system that differs from traditional planning optimization to build all components. The repowering strategy is to integrate wind turbines (WTs) and battery into the original system. For the repowering system, a power management strategy is proposed to determine the operating modes of the PHS and battery. Three objectives, which are minimizing percentage of the demand not supplied, levelized cost of energy, and curtailment rate of renewable energy, are considered in the optimization model. Simulation is conducted by single-objective, biobjective, and triobjective particle swarm optimization (PSO) techniques. For the single-objective optimization, the comparison of PSO and genetic algorithm (GA) is made. For the double-objective optimization, multiobjective PSO (MOPSO) is compared with weighted sum approach (WSA), and fuzzy satisfying method is utilized to find the win-win solution. The results reveal that the repowering strategy can help to achieve maximum reliability of power supply after load demand increases significantly, and the battery plays an important role in such a hybrid system.

KEYWORDS

multiobjective optimization, particle swarm optimization, power management strategy, PV-PHS hybrid system, repowering optimization

1 | INTRODUCTION

In the last 20 years, global wind power and photovoltaic (PV) power installed capacity increased from 7.64 to 468.99 GW and from 0.23 to 301.47 GW, respectively. Wind and PV power generation have grown rapidly, increasing 79-fold to 959.5 TWh and 439-fold to 331.1 TWh, respectively.[1] However, renewable power generation, such as

wind and PV power generation, will cause great disturbance to the power grid if connected to the grid directly, since it has the disadvantage of fluctuation and intermittence.[2,3] In general, a hybrid energy system is a combination of different renewable energy sources and storage devices, which can not only effectively alleviate the disturbance to the power grid caused by renewable energy generation but also greatly reduce the phenomenon of curtailment of wind and solar.[4,5] Many storage devices have been applied in hybrid systems.[6,7] Pumped hydro storage (PHS) is a preferable storage device, with low cycle cost, and is considered the most mature technology.[8] Several hybrid energy systems have been built in the world to date. In 2017, French company C&T International constructed a PV-PHS hybrid system using floating PV panels in Portugal, which is reported in the newspaper (*Energy Monitor Worldwide*). China has the world's largest PV-PHS hybrid system in Longyangxia, with an installed hydropower capacity of 1280 MW and a PV installation capacity of 850 MW.[9]

In addition to these practical applications, there is an extensive research on the planning optimization of various types of the hybrid energy systems. Several papers in the literature present different methods for sizing optimization.[10-13] Techno-economic model was used to design the hybrid energy system including PV, wind turbine, battery bank, and diesel generator based on genetic algorithm (GA).[10] A dynamic multiobjective particle swarm optimization (MOPSO) was presented for designing the hybrid energy systems aiming to minimize simultaneously the total net present cost, unmet load, and fuel emission.[11] A simple method for designing the hybrid renewable energy systems might adopt HOMER software, which is a powerful tool for planning optimization.[14] For multiobjective optimization problems, Pareto front was usually used to address the trade-off. But it could not give the win-win result. ε-contraint method[15] and weighted sum technique[16] were employed to solve the multiobjective optimization model that could obtain the Pareto front, and then fuzzy satisfying technique was used to find the win-win solution in the Pareto front. These studies on planning optimization were mainly related to build a new system. For the already-built standalone systems, the existing hybrid energy systems need to be ameliorated when mismatch occurs between electricity supply and load demand. This study focuses on the existing standalone hybrid system and its repowering strategy. Such strategy allows to identify and integrate new components into the existing system and provide optimized solutions to eliminate the mismatch between supply and demand.

The methods discussed above in newly built systems are also applicable for the existing hybrid energy systems. Repowering optimization, which is often called expansion planning, has been applied in various existing energy system. Hou et al[17] study the methods of expansion planning for the existing district energy systems in China to address the problems of low efficiency and insufficient energy supply. A combined socioeconomic model is proposed in Candas et al[18] to investigate German and Italian PV future expansion without consideration of feed-in tariffs. In ZekiYılmazoğlu et al,[19] solar repowering of an existing thermal power plant is analyzed by conducting simulations. When taking CO_2 taxes into account, the proper option of repowering the existing thermal power plant is integrating solar energy. In Serri et al,[20] from the perspective of technical-economic assessment, the evaluation of the repowering potential of wind energy plants in Italy is discussed by means of three steps methodology, and this paper could be a starting point for a more global analysis to the future of wind energy in Italy. Hou et al[21] is the first paper to investigate the profitability of the repowering strategy by means of adaptive PSO, and the authors focus on optimization of offshore wind farm repowering using the evaluation index of the levelized cost of energy (LCOE).

Through widely reading literatures, no research has been found for repowering optimization of an existing standalone hybrid energy system. Therefore, this paper applies repowering optimization to an existing standalone PV-PHS hybrid system, which is one option when the original system cannot meet the increased load demand. Wind turbines and batteries are selected to be integrated into the system. Integrating diesel engines is also a solution, but it can cause a lot of pollution.[22,23] Therefore, the solution of integrating diesel engines is not considered in this research.

It is worth mentioning that this research is based on a real system located in Xiaojin, Sichuan, China. Working

Novelty Statement

- The concept of reconstructing a photovoltaic-pumped hydro storage (PV-PHS) hybrid system is proposed based on a real PV-PHS hybrid system in Xiaojin, Sichuan, China. To the best of our knowledge, it is the first study to investigate reconstructing an existing standalone PV-PHS hybrid system; the proposed concept and methods are applicable to other hybrid systems.
- A power management strategy is introduced and examined to manage operating modes of PHS and batteries to reduce the usage of battery and extend its lifetime.
- A triobjective optimization model with consideration of system reliability, the investment cost, and the curtailment rate of renewable energy is constructed and simulated.

on a real case offers the potential solutions to repowering the system and facilitate the local planners to make decisions.

The contributions of this paper can be summarized as follows:

1. The concept of reconstructing a PV-PHS hybrid system is proposed based on a real PV-PHS hybrid system in Xiaojin, Sichuan, China. To the best of our knowledge, it is the first study to investigate reconstructing an existing standalone PV-PHS hybrid system; the proposed concept and methods are applicable to other hybrid systems.
2. A power management strategy (PMS) is introduced and examined to manage operating modes of PHS and batteries to reduce the usage of battery and extend its lifetime.
3. A triobjective optimization model with consideration of system reliability, the investment cost, and the curtailment rate of renewable energy is constructed and simulated.

The following sections are organized as follows. Section 2 presents the mathematical models for each component and the objective function used in this research. Section 3 describes the optimization algorithm, including MOPSO and fuzzy satisfying method, and the PMS. Section 4 analyzes the original system and the proposed repowering strategy. Finally, Section 5 summarizes results and the comprehensive analysis of this research.

2 | MATHEMATICAL MODELS

The repowering of a PV-PHS hybrid system is investigated in the research that is based on a real system in Xiaojin, Sichuan, China (latitude: 30.76477°, longitude: 102.11929°). The schematic diagram of the original and new system in Xiaojin, Sichuan, China, is given in Figure 1. The studied area is marked in Figure 1 by a red circle. Xiaojin is located in the northwest of Sichuan Province with abundant water resources and solar irradiation, and its geographical location is relatively remote. According to the local environmental and geographical conditions, a standalone PV-PHS hybrid energy system was built to serve local electricity users, which is the original system in the research. The original system can completely meet the local load demand in the first few years. It consists of PV array, converter, load, local substation, upper and lower reservoirs, pump, and water turbine. When there is solar radiation in the daytime, the PV array generates power to the load and the surplus power is stored in the PHS. At night, only the PHS generates power to the load. The blue and black arrows in the Figure 1 indicate the direction of water and power flow, respectively. However, in recent years, with the rapid economic growth, the load demand and profile change greatly, and the original system cannot fully meet the local load demand since sometimes the shortage of power supply and power outages will occur. Therefore, the original system should be reconstructed to fulfill the local load. The reconstructed system is the new system as shown in Figure 1. According to the project requirements, the new

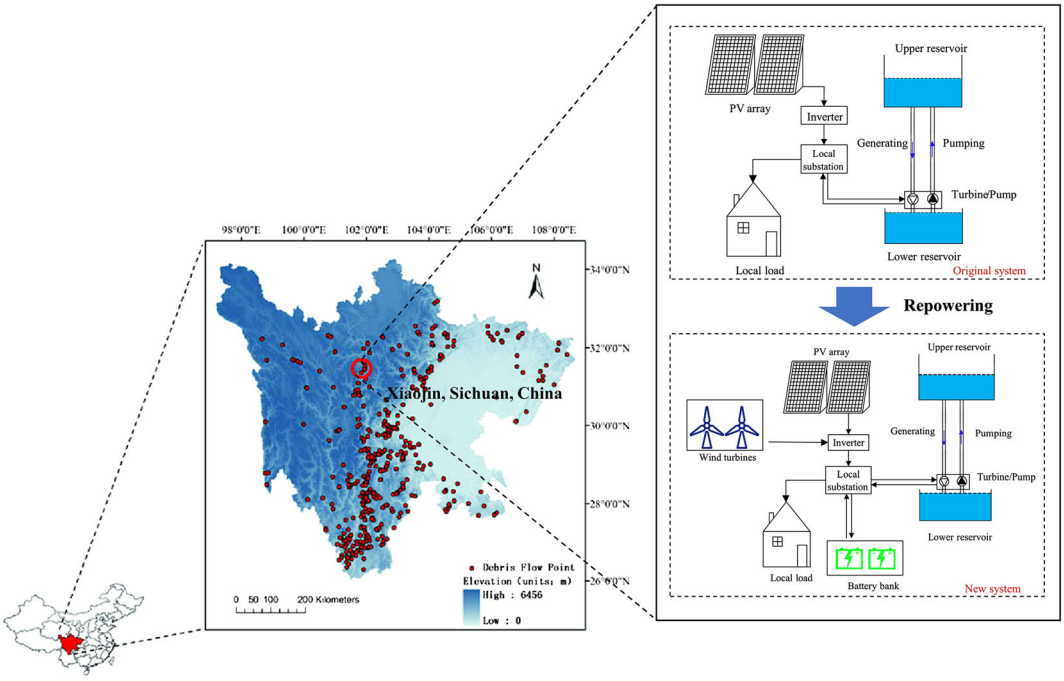

FIGURE 1 The schematic diagram of the original and new system in Xiaojin, Sichuan, China [Colour figure can be viewed at wileyonlinelibrary.com]

system needs to meet the load demand in 5 years. Besides, due to the policy requirements, the new system takes the curtailment rate of renewable energy into consideration. The wind power is considered to provide adequate electricity because the limited area cannot install more PV array. Since replacing a new pump/water turbine is not cost-effective and will take a long time, and a small capacity of storage devices can help to meet the load demand, the battery as an auxiliary energy storage equipment for the PHS is considered. The operating modes of PHS and battery are determined by the PMS, and its detailed description is given in the latter section. The following sections present the models used in this research, which contains wind turbines, PV array, PHS, and battery bank. In addition, the model of the objective function is also included.

2.1 | Power output model of PV array

The output power of PV array is affected by many factors. The radiation intensity directly determines the PV output. The influence of temperature cannot be ignored since the power generation efficiency of the PV array decreases with an increase in temperature. In this paper, PV output takes the influence of temperature into account. The formula of PV array output considering the temperature effect can be written as[24,25]

$$P_{PV} = N_{PV}\eta_{inv}P_R\frac{G_T}{G_{ref}}[1 + k_P(T_C - T_{ref})], \quad (1)$$

$$T_C = T_{amb} + (0.0256 \times G_T). \quad (2)$$

2.2 | Power output model of an individual wind turbine

There are many models in the literature for calculating the output power of an individual wind turbine. However, plenty of literature estimates the output power of wind turbines without considering variation in wind speed at different vertical heights. The wind speed at the installation height should be estimated from the reference wind speed measured by the meteorological station. The power output curve, wind speed, and tower height are the three main factors determining the output power of wind turbines. The formula for output power of an individual wind turbine can be expressed as[26,27]

$$P_{WTout} = \begin{cases} 0 & V < V_{ci} \\ \frac{P_{WTR}}{{V_R}^3 - {V_{ci}}^3}\cdot V^3 - \frac{{V_{ci}}^3}{{V_R}^3 - {V_{ci}}^3}\cdot P_{WTR} & V_{ci} \le V < V_R \\ P_{WTR} & V_R \le V < V_{co} \\ 0 & V > V_{co} \end{cases}, \quad (3)$$

$$V = V_{ref}\cdot\left(\frac{H_{WT}}{H_{ref}}\right)^{\lambda}. \quad (4)$$

2.3 | Pumped hydro storage

PHS stores surplus energy as potential energy by pumping water from a lower reservoir to the upper one. The water in the upper reservoir (UR) will be released to generate power when an energy deficit occurs. According to previous literature, the design parameters of the PHS include the capacity of the reservoirs, the height difference of the PHS, the sizing of pumps, and water turbines. All the parameters mentioned above are known in the original system. The PHS consists of a variable-speed pump, a water turbine, and an UR, which are modeled as follows[28]:

2.3.1 | Generating mode

During discharging mode, the water turbine power output can be written as

$$P_w = \eta_w\rho g h q_w. \quad (5)$$

In fact, the overall efficiency of the water turbine changes with operating conditions. In this paper, the overall efficiency is considered to be a fixed value.

2.3.2 | Pumping mode

A variable-speed pump is installed in the original system that works if available power is more than 10% of its maximum power. The electricity input for the pump is from the PV array in the original system and the PV array and wind turbines in the repowered systems. The water volumetric flow rate output from the pump can be written as

$$q_p = \frac{\eta_p P_p}{\rho g h}. \quad (6)$$

2.3.3 | Upper reservoir

The main factors that influence the water quantity of the UR are charging and discharging. Water loss in the UR includes evaporation, leakage, and precipitation, which is evaluated by introducing $1 - \beta$. The effect of rainfall on the UR is not considered in this paper for simplification. The water quantity of the UR at hour t can be expressed as

$$Q_{UR}(t) = (1 - \beta)Q_{UR}(t-1) + \int_{t-1}^{t} q_p(t)dt - \int_{t-1}^{t} q_w dt, \quad (7)$$

where $Q_{UR}(t)$ and $Q_{UR}(t-1)$ are associated state variables. The available water quantity of the UR is determined by

the capacity of UR, which is restricted by

$$0 = Q_{\mathrm{UR,min}} \le Q_{\mathrm{UR}} \le Q_{\mathrm{UR,max}} = V_{\mathrm{UR}}. \quad (8)$$

In this paper, the minimum water quantity of the UR $Q_{\mathrm{UR,min}}$ is set to 0.

2.4 | Battery bank

The power generated from the PV array and wind turbines at each hour not only determines the pumping/releasing of water to/from the UR but also determines the charge/discharge state of the battery bank. The battery bank is a new component for the original system, which serves as a backup storage device for the PHS. The charging-discharging process should be reduced to prolong the service life of the battery bank. In reality, the response time of the battery bank and PHS is very different, and the battery bank has a shorter response time. However, the effect of response time is ignored in this study. The energy stored in the batteries can be regarded as a state variable to illustrate the operation of the battery bank, which is formulated using the following dynamic equation[29]

$$E_{\mathrm{Bat}}(\mathrm{t}) = E_{\mathrm{Bat}}(\mathrm{t}-1) + (1-x)P_{\mathrm{ch}}\eta_{\mathrm{ch}} - x\frac{P_{\mathrm{dis}}}{\eta_{\mathrm{dis}}}, \quad (9)$$

where $x = 0/x = 1$ means the battery bank is in charge/discharge state. The binary decision variable x is introduced in this paper to consider the physical constraint of the battery bank and in order to avoid the battery bank charging and discharging at the same time.

Changes in available energy stored in the battery bank are mainly caused by its charge/discharge behaviors; however, the available energy is bounded by the limits of the battery state of charge ($\mathrm{SOC_{min}}$ and $\mathrm{SOC_{max}}$), which is subject to the following constraints[30]:

$$\mathrm{SOC_{min}}\cdot E_{\mathrm{Bat,max}} \le E_{\mathrm{Bat}} \le \mathrm{SOC_{max}}\cdot E_{\mathrm{Bat,max}}, \quad (10)$$

$$\mathrm{SOC_{min}} = 1 - \mathrm{DOD}. \quad (11)$$

DOD means the depth of discharge, which is applied to show how deeply the battery bank is discharged.

In this paper, the capacity and charge/discharge power of the battery bank are both designed as optimization variables in repowering strategy, and the charging power is equal to the discharging power. Therefore, the constraints of charge/discharge power at hour t can be written as

$$0 \le P_{\mathrm{ch}} \le P_{\mathrm{bat\_max}}, \quad (12)$$

$$0 \le P_{\mathrm{dis}} \le P_{\mathrm{bat,max}}. \quad (13)$$

2.5 | Modeling of the PDNS

The percentage of the demand not supplied (PDNS) means the ratio of unsatisfied load to total load in a year[31] which is the first objective function and should be minimized. It can be used to evaluate the reliability of the hybrid system, which is regarded as a constraint condition in this research. For the original system and repowering strategy, the equations of calculating the PDNS are different since the load demand is supplied by different components. For original system, load demand is supplied by PV array and PHS (Equation 14). Load demand is provided by PV array, wind turbines, battery bank, and PHS for the repowering strategy (Equation 15).

$$PDNS = \min\left\{\sum_{t=1}^{8760}\frac{P_{\mathrm{PV}}(\mathrm{t}) + P_{\mathrm{w}}(\mathrm{t}) - P_{\mathrm{load}}(t)}{P_{\mathrm{load}}(t)}\times 100\%\right\} \quad (14)$$

$$PDNS1 = \min\left\{\sum_{t=1}^{8760}\frac{P_{\mathrm{PV}}(t) + P_{\mathrm{WT}}(t) + P_{\mathrm{w}}(t) + P_{\mathrm{dis}}(t) - P_{\mathrm{load}}(t)}{P_{\mathrm{load}}(t)}\times 100\%\right\} \quad (15)$$

2.6 | Economic model

The economic model is to optimize the components of the repowering strategy, including the number of wind turbines (N_{WT}), the capacity of the battery bank ($E_{\mathrm{Bat,max}}$), and the charge/discharge power of the battery bank (P_{max}). Plenty of literature takes techno-economic index as objective function.[32,33] For the single-objective analysis, it can be regarded as a subset of Pareto front in

$$\mathrm{LCOE} = \min\left\{\frac{CRF\cdot\sum_{i=0}^{y}\left[\frac{C_{\mathrm{cap\_bat}} + C_{\mathrm{main\_bat}} + C_{\mathrm{rep\_bat}} + C_{\mathrm{cap\_wt}} + C_{\mathrm{main\_wt}} + C_{\mathrm{rep\_wt}}}{(1+i)^y} - SV\right]}{E_{\mathrm{served}}}\right\}. \quad (16)$$

techno-economic biobjective optimization, since the premise of the minimum cost is to ensure the maximum reliability, which means avoiding demand not supplied. The second objective aims to minimize the LCOE, which is an excellent indicator to evaluate the economic feasibility of the repowering strategy, and can be written as[34]

CRF is applied to annualize the investment cost; the capital recovery factor can be formulated as

$$CRF = \frac{i \cdot (1+i)^{y}}{(1+i)^{y} - 1}. \tag{17}$$

The formula to calculate the discount interest rate is offered below.

$$i = \frac{i' - f}{1+f} \tag{18}$$

For the repowering system, the revenues are the salvage value (SV) of battery and wind turbines that happens at the end of the project lifetime. Based on the initial or replacement costs, it can be written as

$$SV = C_{\text{rep}} \cdot \frac{N_{\text{rem}}}{N_{\text{life}}}. \tag{19}$$

2.7 | Curtailment rate

The PHS and battery in the repowering system stores surplus electricity, but the power provided by PV arrays and wind turbines is restricted by the capacities of the storage devices. Therefore, the curtailment of PV and wind power would occur since the PV array and wind turbines cannot reach its maximum power output when it is more than the sum of load demand and the energy storage capacities. CR is defined as the curtailment rate of the PV and wind power that cannot be supplied to the load and stored in the storage devices. The third objective aims to minimize the CR, which can be formulated as

$$CR = \min\left\{ \frac{\sum_{t=1}^{8760} [P_{\text{WT}}(t) + P_{\text{PV}}(t) - P_{\text{offer}}(t)]}{\sum^{8760} [P_{\text{WT}}(t) + \text{P}_{\text{PV}}(t)] \cdot 100\%} \right\}. \tag{20}$$

2.8 | Characterization of uncertain PV and wind power

Since the new planning system needs to meet the load demand in 5 years, the uncertainties of PV and wind power are modeled by means of the forecast error. The uncertain PV and wind power are defined as[35,36]

$$P_{\text{PV}}^{\text{u}} = P_{\text{PV}} + e_{\text{PV}}, \tag{21}$$

$$P_{\text{WTout}}^{\text{u}} = P_{\text{WTout}} + e_{\text{WT}}. \tag{22}$$

For the stochastic optimization, it is widely accepted that the forecast errors of uncertain parameters obey a normal distribution:

$$e_{\text{PV}} \sim N(u_1, \sigma_1^2), \tag{23}$$

$$e_{\text{WT}} \sim N(u_2, \sigma_2^2). \tag{24}$$

3 | REPOWERING STRATEGY OPTIMIZATION

3.1 | PMS of the PHS and battery

The PMS is proposed to regulate energy distribution among energy storage systems (PHS and battery), power sources (PV and wind power), and load. Therefore, the PMS decides how the hybrid energy system works and its key variables vary. The PMS is designed to address the complex operation problems of the PHS and battery in this research. Due to the high investment cost and short lifetime of the battery, the battery as an auxiliary storage device operates after the PHS works. The operating modes depend on the surplus power generated from the PV array and wind turbines (P_s), the UR level ($0 < Q_{\text{UR}} < V_{\text{UR}}$), and the SOC of the battery ($\text{SOC}_{\min} < \text{SOC} < \text{SOC}_{\max}$). The flowchart of the PMS is given in Figure 2, which presents the detailed operation strategy of PHS and battery.

If surplus power $P_s < 0$, the UR level Q_{UR} and the SOC of the battery are checked. If UR level $Q_{\text{UR}} > 0$, the PHS provides electricity to the load. When load demand is over the maximum output of the PHS and UR level $Q_{\text{UR}} > 0$, the battery is used to meet the load demand. If the load demand is greater than the sum of the maximum output of the water turbine and battery, the load loss occurs, which should be eliminated or reduced. If UR level $Q_{\text{UR}} < 0$ and battery $\text{SOC} > \text{SOC}_{\min}$, only the battery bank supplies electricity to satisfy the load.

If surplus power $P_s > 0$, the UR level Q_{UR} and the SOC of the battery are checked again. In case of UR level $Q_{\text{UR}} < V_{\text{UR}}$ and $P_s > 10\%$ of the maximum power of pump, the surplus power is first used to pump the water from lower reservoir to the upper one, and if the pump is working at its maximum power and battery $\text{SOC} < \text{SOC}_{\max}$, the rest of electricity is charged by the battery bank. When the surplus electricity is more than the sum of the maximum output of pump and battery, it will be wasted, which leads to the curtailment rate of PV and wind power. If

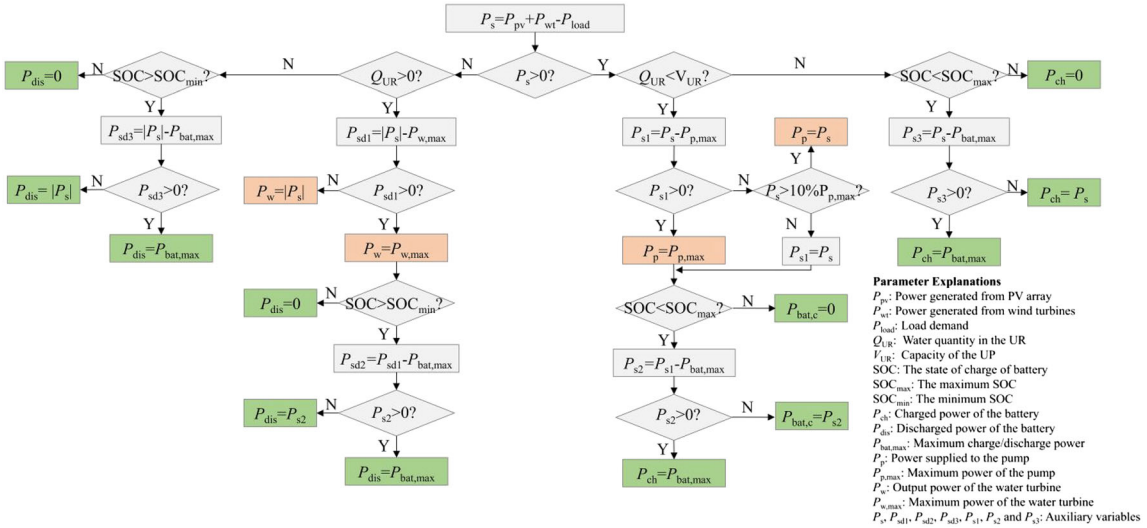

FIGURE 2 Flowchart of the power management strategy (PMS) [Colour figure can be viewed at wileyonlinelibrary.com]

the UR level $Q_{UR} > V_{UR}$ and battery SOC < SOC_{max}, the available power is used to charge battery.

3.2 | Particle swarm optimization

At present, plenty of evolutionary algorithms, with a good chance of obtaining the optimal solution for a nonlinear optimization problem, have been used to replace mathematical algorithms in the literature. Among these, GA and PSO are extensively used. Due to the excellent performance of PSO in computational efficiency,[37] it is chosen to conduct the simulations in this research. Single-objective optimization can be achieve using original PSO. For the multiobjective optimization, the MOPSO can be used to find the Pareto-optimal front. Abido[38] gives a detailed description of MOPSO, and the main steps of MOPSO are shown below:

Step 1: Initialize population according to the size of populations and the value range of the optimization variables.
Step 2: Sort initial population according to nondomination.
Step 3: Find best populations including local best and global best.
Step 4: Start from first generation to implement the following five procedures for each iteration:
1. Update each particle velocity and position according to the local best and global best.
2. Evaluate the objective functions using the updated particle position.
3. Search for nondominated solutions.
4. Expand and update nondominated global and local set.
5. Find the new best populations to update the previous one.

Step 5: Update the weight and learning factor, and then repeat Step4 until the stop criteria satisfied.

In this paper, the number of particles and the maximum number of generations are set to be 100 and 200, respectively. The extension factor of solution set of nondominated solutions is 0.1. Both selection factors and elimination factors of nondominant solutions are 2. A framework of the optimization design for the repower strategy is given in Figure 3.

3.3 | Fuzzy satisfying method

For the multiobjective optimization, the MOPSO obtains many different solutions. The fuzzy satisfying approach can be employed to select the win-win result amid the obtained solutions, which normalizes the objectives.[15] In order to obtain the win-win result, the objective functions of LCOE and PDNS are modeled using membership functions. The solution satisfaction depends on the values of the membership functions. The membership function is calculated under the lower and upper limits of ith objective function. The membership function for the nth solution of ith objective function is defined as follows[39]:

$$\phi_i^n = \begin{cases} 1 & \phi_i^n \le \phi_i^{\min} \\ \dfrac{\phi_i^{\max} - \phi_i^n}{\phi_i^{\max} - \phi_i^{\min}} & \phi_i^{\min} \le \phi_i^n \le \phi_i^{\max} \\ 0 & \phi_i^n \ge \phi_i^{\max} \end{cases}. \quad (25)$$

The fuzzy solutions can be obtained by Equation (26) for the fuzzy multiobjective. Then, the maximum weakest

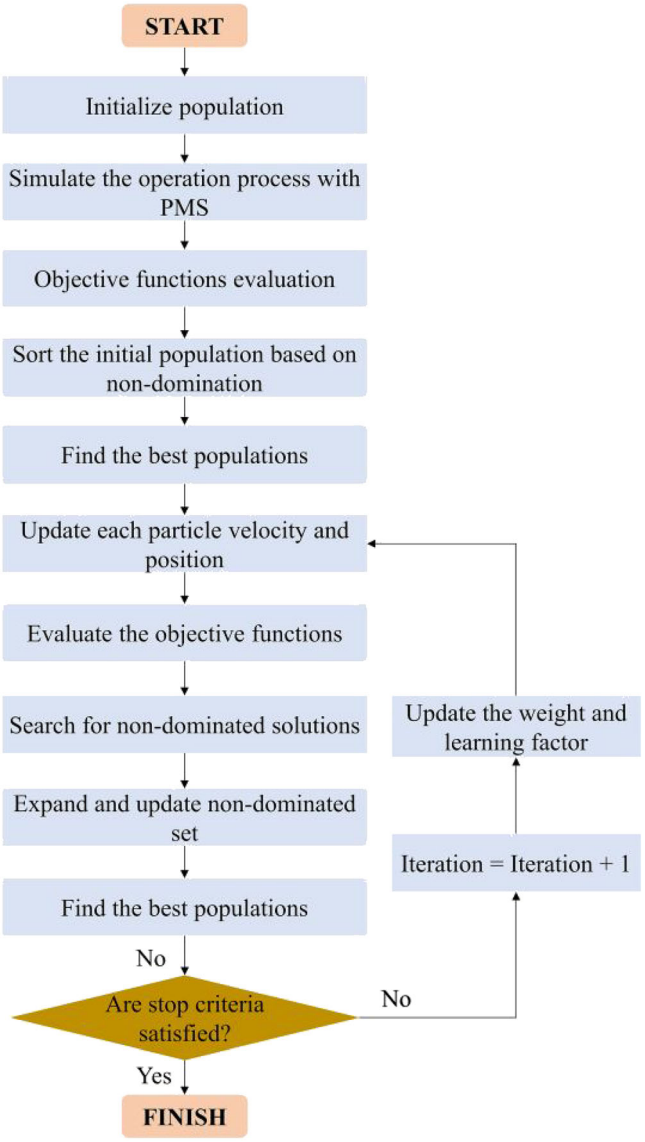

FIGURE 3 The optimization framework using multiobjective particle swarm optimization (MOPSO). PMS, power management strategy [Colour figure can be viewed at wileyonlinelibrary.com]

membership function is calculated using Equation (27), which is considered as the win-win solution.

$$\phi^n = \min\left(\phi_1^n, ..., \phi_N^n\right) \tag{26}$$

$$\phi^{\max} = \max\left(\phi^1, ..., \phi^N\right) \tag{27}$$

4 | RESULTS

4.1 | Data

The research investigates a PV-PHS hybrid energy system repowering in Xiaojin, Sichuan, China (latitude: 30.76477°, longitude: 102.11929°) as case of study, which is marked in Figure 4 (red dot). The meteorological data that contains hourly temperature, hourly solar irradiation, and hourly wind speed is shown in Figure 4. For the new load demand, the battery and wind turbines are used to repower the original system. The battery can be regarded as the auxiliary storage to assist the PHS in order to completely satisfy the new load demand. Two different batteries (lead-acid and Li-ion battery) are selected to conduct the simulation, and their specification information is given in Table 1. The wind turbines can generate adequate power and then provide it to the new load demand. The detailed information of the selected wind turbine is shown in Table 2.

4.2 | The original system

The original system is a PV-PHS hybrid energy system that is a real case located in Xiaojin, Sichuan, China. The original system consists of PV arrays (40154 kWp) and the PHS (UR: 559810 m^3, pump: 9500 kW, water turbine: 6120 kW). According to the information, the research investigates the performance of the original system and the feasibility of the repowering strategies after the increase of load demand. Based on the meteorological data, the PV model adopted in this research and the known PV construction number, the monthly total output power of PV array in a year is obtained (see Figure 5). From March to August, PV output is relatively high due to the intense solar radiation. The maximum and minimum monthly average PV output in a year occur in July and December, respectively. Figure 6 gives the present and future monthly total load demand in a year. The future load demand (5 years later) is 1.4 times that of the present which is the prediction results from the State Grid Sichuan Company. It can be observed that the load demand in spring and winter is high, while load demand is low in summer and autumn. Since the selected site is located in the plateau with a relatively low temperature in summer.

Figures 7 and 8 give the demand not supplied at present and in the future, respectively. Under the present and future load demand, the original system cannot totally meet the load demand. At present, the original system leads to 3.8% of the demand not supplied and the demand not supplied occurs in winter and spring due to the high load demand. The curtailment rate of the PV power reaches 35.6%. In the future, due to the higher load demand, more load demand cannot be met and the original system will cause 18.4% of the demand not supplied. The condition of demand not supplied becomes more serious comparing with the present condition. The curtailment rate of the PV power reduces to 9.9%. For some areas, the reliability requirement of the load is relatively high, namely, the load must be completely supplied.

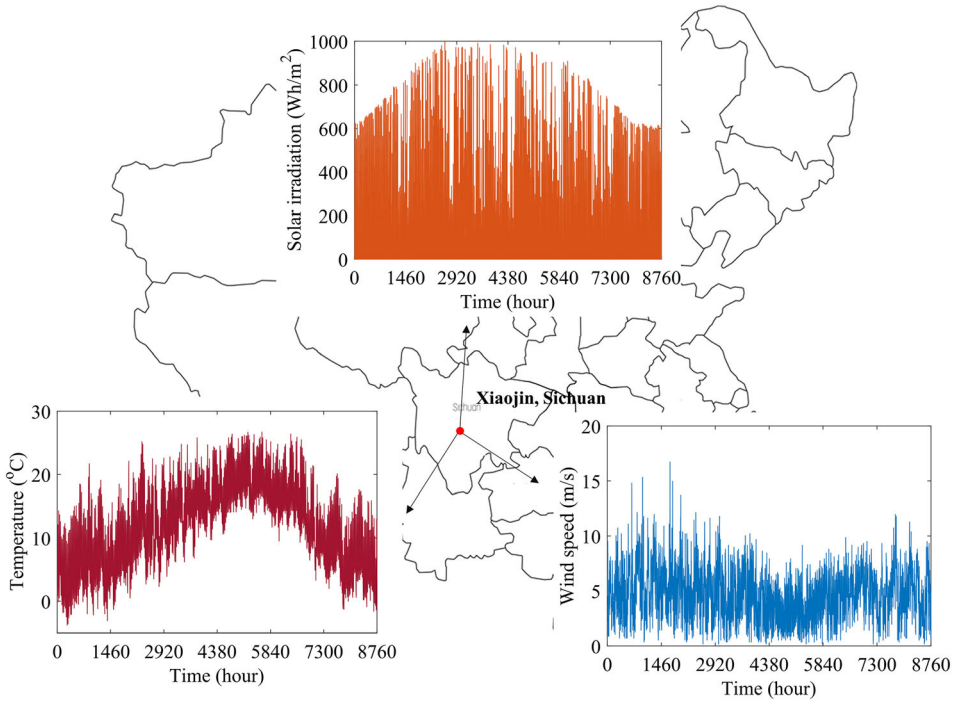

FIGURE 4 Meteorological data in Xiaojin, Sichuan, China [Colour figure can be viewed at wileyonlinelibrary.com]

TABLE 1 The specification of different battery[40]

	Lead-Acid Battery	Li-Ion Battery
Lifetime, y	10	15
Roundtrip efficiency, %	90	95
DOD, %	80	80
SOC_{max}	100	100
Capital cost per power, $/kW	800	1000
Capital cost per capacity, $/kWh	500	1500
Operating and maintenance cost, $/kW/y	8	10
Replacement cost, $/kWh	500	1500

TABLE 2 The specification of wind turbine[41]

Parameters	Value
Rated power, kW	250
Cut-in wind speed, m/s	2.5
Cut-out wind speed, m/s	8
Rated wind speed, m/s	20
Capital cost, $/unit	375 000
Operating and maintenance cost, $/unit/y	7500
Replacement cost, $/unit	265 500
Lifetime, y	20

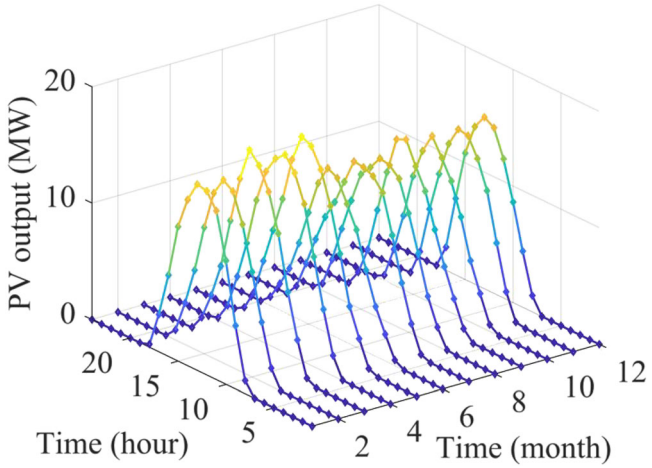

FIGURE 5 Monthly total photovoltaic (PV) output [Colour figure can be viewed at wileyonlinelibrary.com]

Therefore, the original system should be reconstructed to meet the load demand.

Through the above analysis, the original system causes a little demand not supplied before the increase of load demand. After the load demand changes in the future, the PV-PHS hybrid system cannot provide enough power to the load; hence, the PV-PHS hybrid system owner should take measures to deal with this issue. Integrating a new power plant and increasing storage capacity may be a good approach to reconstruct the original system to meet the new load demand. Therefore, this paper proposes a repowering strategy, which is the integrating

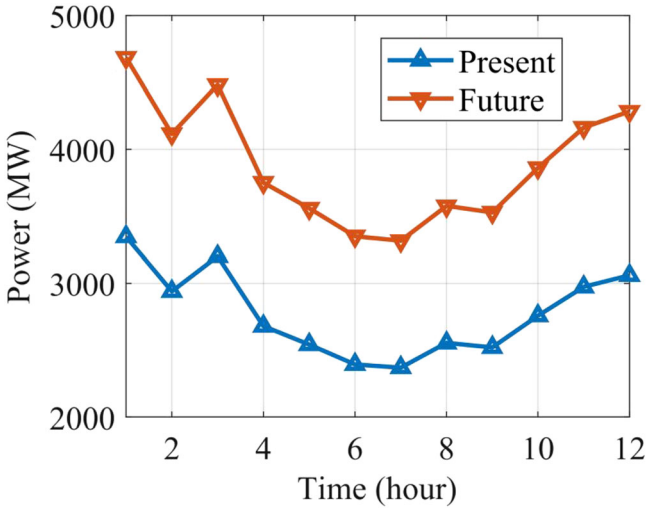

FIGURE 6 Present and future monthly total load demand [Colour figure can be viewed at wileyonlinelibrary.com]

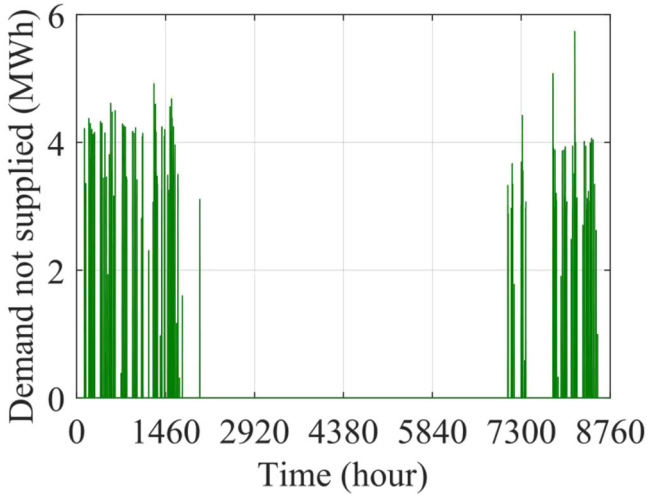

FIGURE 7 Hourly demand not supplied at present [Colour figure can be viewed at wileyonlinelibrary.com]

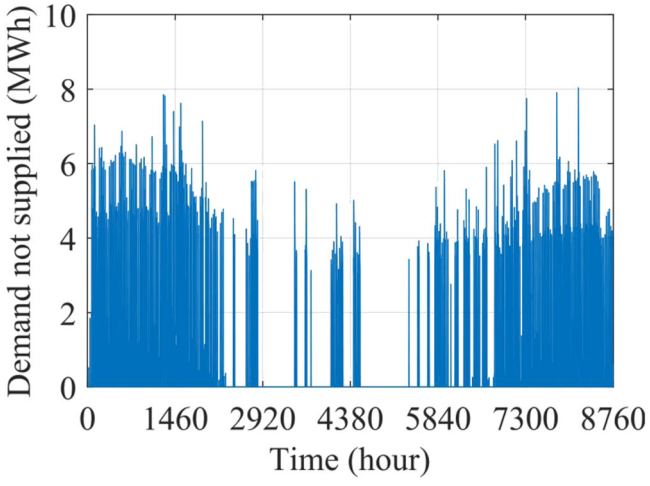

FIGURE 8 Hourly demand not supplied in the future [Colour figure can be viewed at wileyonlinelibrary.com]

WTs and battery repowering strategy with practical reference value. It can be observed that the repowering strategy integrates wind turbines so the daily average output power of an individual wind turbine in a year is given in Figure 9. This is calculated using the meteorological data and the wind turbine model adopted in this research. The total wind turbine output depends on optimization results of the number of wind turbines. Based on the PV output data, new load demand, and an individual wind turbine output, the repowering strategy is analyzed below.

4.3 | Integrating WTs and battery repowering strategy

Integrating WTs and battery repowering strategy, which makes no changes to the original system, is to integrate wind turbines and battery bank. The wind turbines can generate more power to the load demand. The function of the battery bank is to increase the storage capacity and charge/discharge power of the original system, which is an auxiliary device to assist the PHS. Under the condition of 0% of the demand not supplied, the optimization results are obtained as shown in Table 3. It can be observed that the optimized sizing of the two types of battery can be regarded as the same, but the LCOE of the Li-ion battery is much higher than that of the lead-acid battery. Considering the low LCOE of the lead-acid battery, the following parts is analyzed based on the results of the lead-acid battery. The benchmark case shows that it cannot reach 0% of the demand not supplied without battery as an auxiliary storage device.

During the single-objective optimization, the optimal capacities are found by PSO. GA, which is widely adopted, is used to compare with the PSO to prove the performance of the PSO. These two numerical experiments aim to minimize the LCOE under zero PDNS,

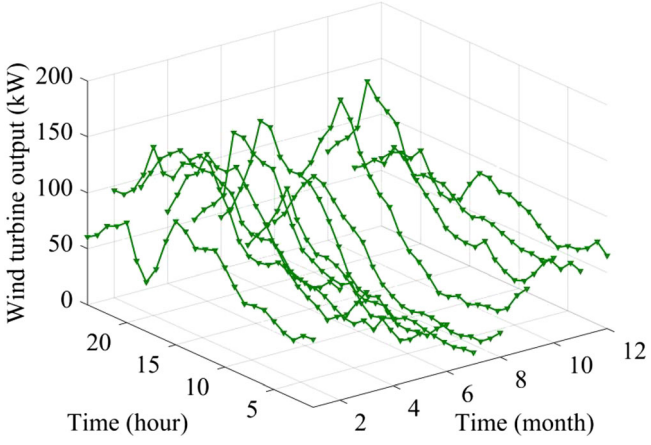

FIGURE 9 Daily wind turbine output [Colour figure can be viewed at wileyonlinelibrary.com]

TABLE 3 The optimized sizing of the two types of battery

	Wind Turbine Number	Battery Power (5 W)	Battery Capacity, kWh	PDNS, %	CR, %	LCOE, $/kWh
Benchmark case	30	0	0	0.62	34	0.0642
Lead-acid battery	30	3001	25 973	0	34	0.1834
Li-ion battery	30	2949	27 242	0	34	0.3184

Abbreviations: PDNS, percentage of the demand not supplied; LCOE, levelized cost of energy; CR, curtailment rate.

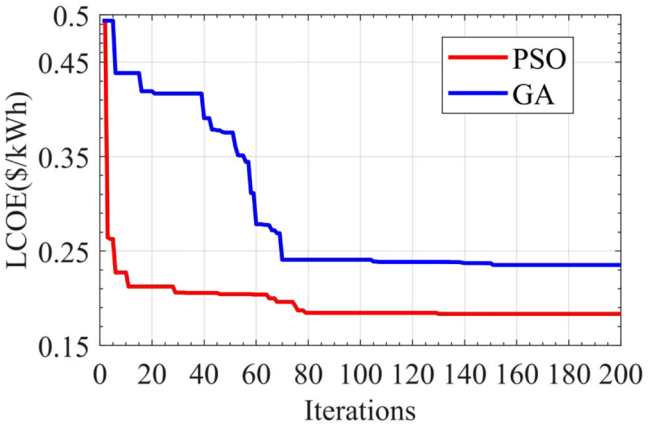

FIGURE 10 Variation of levelized cost of energy (LCOE) during genetic algorithm (GA) and particle swarm optimization (PSO) [Colour figure can be viewed at wileyonlinelibrary.com]

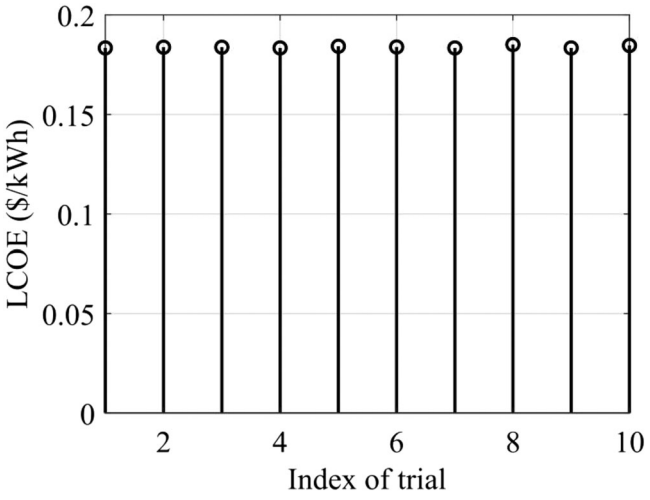

FIGURE 11 The fitness value of ten times trials

and the number of the total iterations are the same. These iteration curves of the two methods are given in Figure 10 . Notably, these two methods are simulated under the same conditions (same initial point). Compared with GA, PSO converges faster and its optimized results are better. Therefore, this paper selects PSO to conduct the simulation. Figure 11 shows the fitness value of 10 times trials of the PSO, which proves its robustness. The LCOE of each trial is close to 0.18 $/kWh. The lowest LCOE is 0.1834 $/kWh, which appears four times in the ten times trials, so this result can be considered relatively accurate.

Figure 12 shows the pumped/released water quantity of the PHS in a year. It can be observed that the PHS sees much more use the battery bank, reducing the number of battery cycles to extend battery life due to the high cost of the battery bank. In Figure 12, the maximum water quantity released corresponding to the rated power of the water turbine is the black dotted line (22 795 m^3) and the maximum water quantity pumped corresponding to the rated power of the pump is the red dotted line (17 275 m^3). In the original system, the rated power of the pump is greater than that of the water turbine, since the PHS needs to store more power from PV array in the daytime and generate electricity to the load by utilizing the energy in the UR at night. Due to the behaviors of the

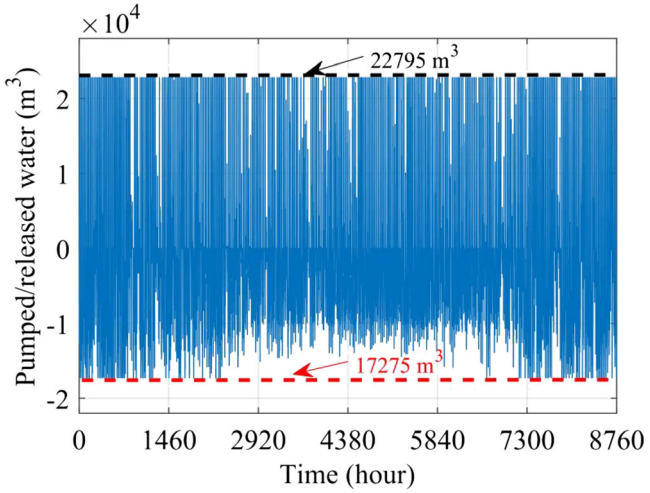

FIGURE 12 Hourly pumped/released water quantity of the pumped hydro storage (PHS) [Colour figure can be viewed at wileyonlinelibrary.com]

pump and water turbine (Figure 12), the water quantity in the UR changes and its changing curve is shown in Figure 13. When the pump/water turbine works to store/generate electricity, the water quantity of the UR increases/reduces. Obviously, in winter and spring, the water quantity of the UR decreases greatly due to the

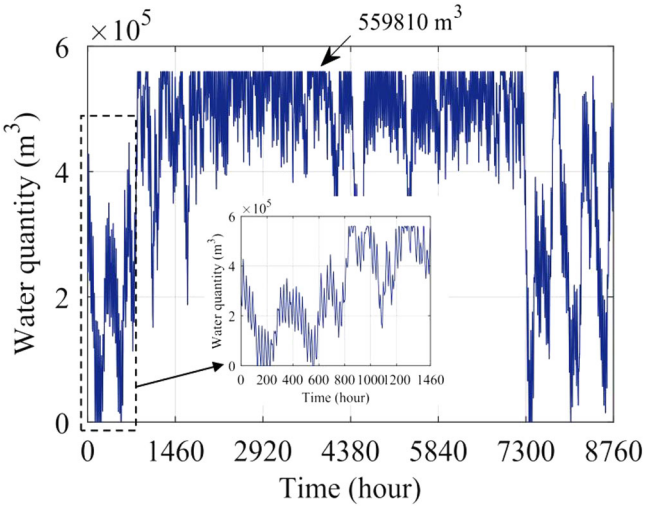

FIGURE 13 The change of water quantity in the upper reservoir (UR) [Colour figure can be viewed at wileyonlinelibrary.com]

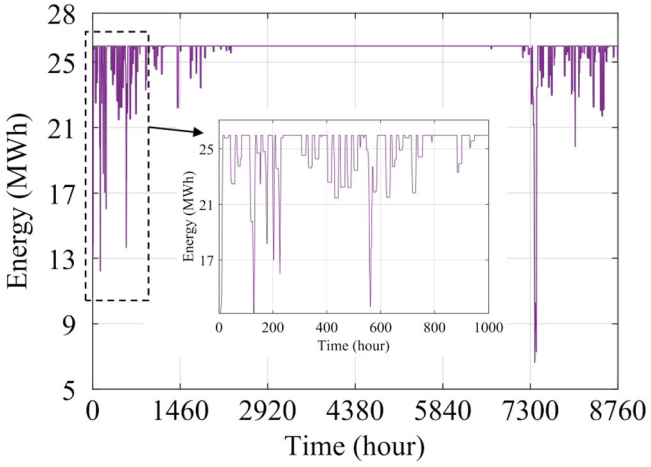

FIGURE 15 The change of energy stored in the battery [Colour figure can be viewed at wileyonlinelibrary.com]

high load demand, and it reaches the lower limit in many hours. The PHS plays a very important role in ensuring the reliability of electricity supply.

Figure 14 gives the charge/discharge power of the battery in a year. Between 2314 and 7170 hours, the battery does not operate because of the high PV generation and low load demand. In the other hours of the year, the battery charges and discharges due to the PHS cannot completely satisfy the new load demand. The changes of energy stored in the battery are shown in Figure 15, and it is related to the behaviors of the battery (Figure 14). When the battery works to charge/discharge electricity, the energy stored in the battery increases/reduces. The energy stored in the battery reaches its lower boundary, which cannot be zero due to its the minimum SOC. As shown in Figures 14 and 15, the behaviors of the battery are relatively rare in a year, but it can ensure the reliability of electricity supply over a year. In fact, battery as an auxiliary storage device does not need to operate frequently since it works when the PHS cannot satisfy the load demand which can extend its lifetime.

To better describe the repowering strategy, under the condition of 0% of the demand not supplied, the simulation results of these two sample days, which can show operation state of the hybrid system with/without the battery participation, are given. The two samples days are 27 January 2017 and 9 July 2017, respectively. For day 1, the battery can assist the PHS to achieve maximum reliability by discharging power to the load. For day 2, the PHS can provide adequate power to the load by itself without the battery participation. The curves of the load demand, wind, and PV power generation in these two sample days are given in Figure 16, and these two sample days are

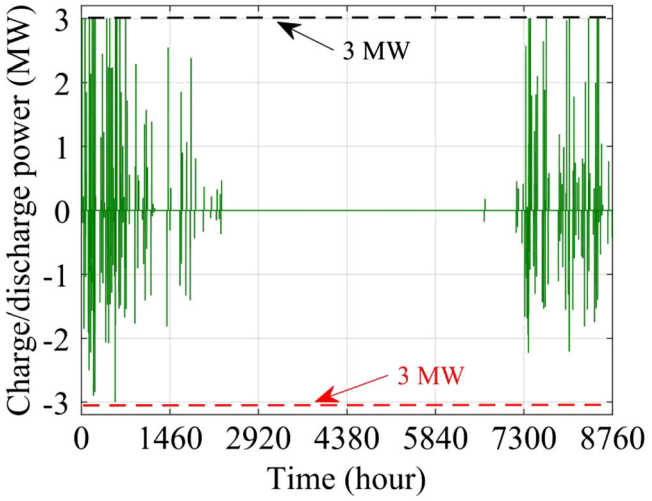

FIGURE 14 Hourly charge/discharge power in the battery [Colour figure can be viewed at wileyonlinelibrary.com]

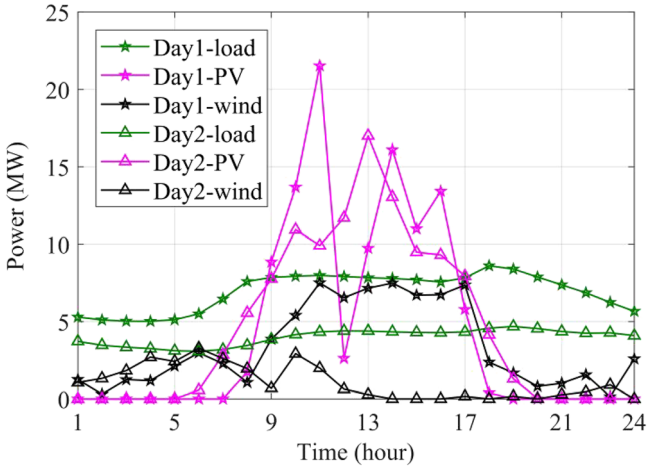

FIGURE 16 The load demand, wind, and photovoltaic (PV) power on these two sample days [Colour figure can be viewed at wileyonlinelibrary.com]

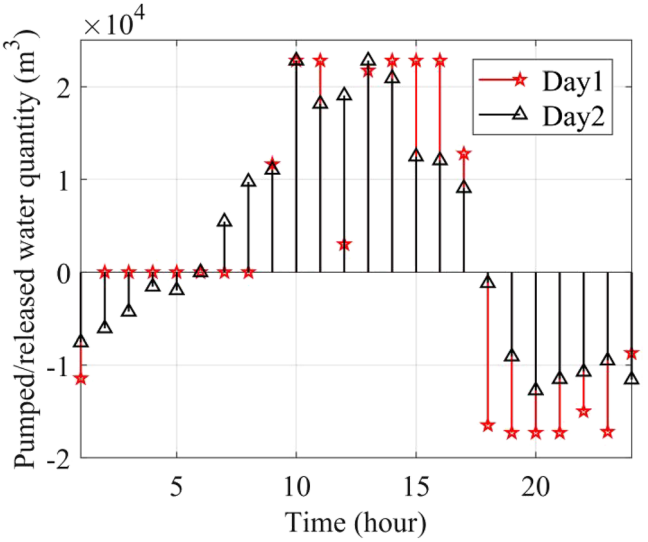

FIGURE 17 The hourly behaviors of the pumped hydro storage (PHS) [Colour figure can be viewed at wileyonlinelibrary.com]

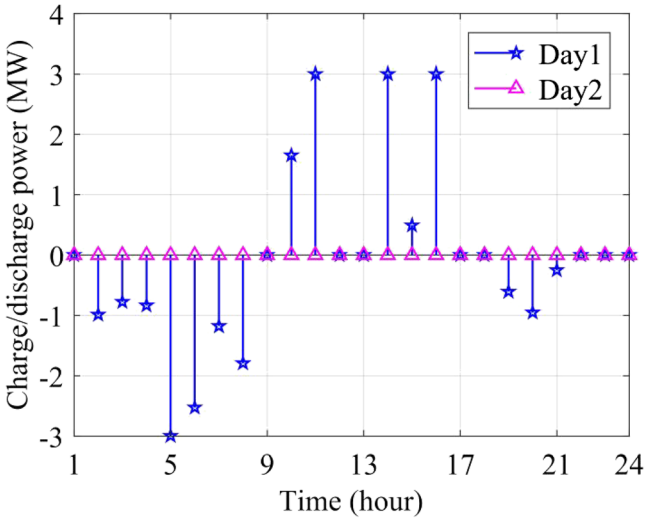

FIGURE 18 The hourly behaviors of the battery [Colour figure can be viewed at wileyonlinelibrary.com]

marked with star and triangle markers, respectively. For these two days, PV can generate sufficient power at the daytime. Comparing with day 1, the hourly load demand and the total wind power of day 2 are lower. Some hours in these two days, the wind power output is greater than the load demand.

Figures 17 and 18 give the hourly pumped/released water quantity of the PHS and hourly charge/discharge power of the battery in these two sample days, respectively. It can be observed that the PHS operates more frequently than the battery since the battery acts as an auxiliary storage device. In Figure 17, for day 1, the PHS pumps from 7:00 to 17:00 due to the enough power generated from the PV array and wind turbines. In other hours, the PHS releases water to generate power to the load. For day 2, the PHS does not work from 2:00 to 9:00 since the water quantity in the UR reaches its lower boundary and the battery provides enough power to the load. In Figure 18, for day 1, the battery charges at the daytime. The battery discharges before 9:00 and after 18:00 since the PHS is empty, which cannot generate power and the water turbine output reaches its rated power, respectively. As shown in Figure 18, it can be observed that the battery does not operate in day 2 since the load demand is low and PHS have the ability to provide enough power to the load. Figure 19 gives the change of the energy in the battery bank and water quantity in the UR of these two days. The curves in Figure 19 depend on the behaviors of PHS and battery in Figures 17 and 18. When the energy in the battery and water quantity in the UR reach their lower or upper limit or the PHS and battery do not work, the curves become flat.

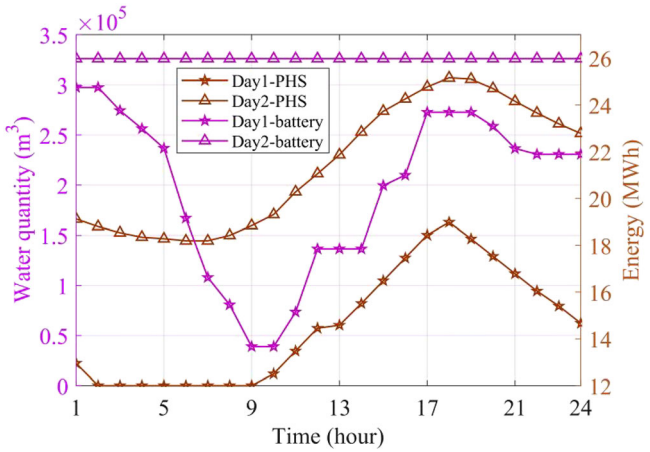

FIGURE 19 The change of energy in the battery and water quantity in the upper reservoir [Colour figure can be viewed at wileyonlinelibrary.com]

The above analysis is based on a single objective (LCOE). Actually, investors can trade off between the LCOE and PDNS in some areas without the high reliability requirement. The two objectives are analyzed by means of the Pareto optimality theory. Figure 20 gives the results of biobjective optimization of the PDNS and LCOE using MOPSO and WSA. Table 4 gives the Pareto optimal solutions obtained by MOPSO. It can be observed that both two methods show excellent performance to obtain the Pareto front. The left-most point is under the condition of 0% of the demand not supplied, which is analyzed above. Changing acceptable PDNS from 0% to 5.38% can bring a dramatic decrease in LCOE (81.6%). Therefore, if a small PDNS is tolerated, significant reductions in costs can be achieved.

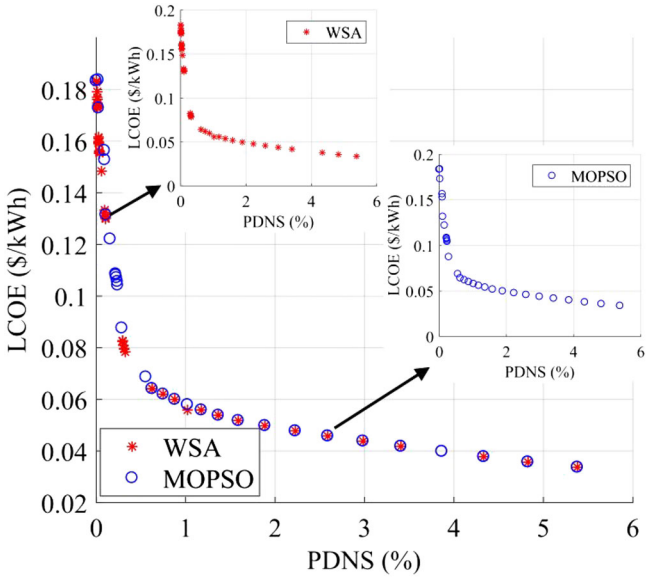

FIGURE 20 Biobjective optimization of the percentage of the demand not supplied (PDNS) and levelized cost of energy (LCOE) [Colour figure can be viewed at wileyonlinelibrary.com]

When the PDNS is zero, maximum reliability is achieved though LCOE is high and the battery bank plays an important role. For some power consumers, such as hospital, manufacturing enterprise, and government departments, the reliability of power supply is more important than the investment cost, and the optimal design under the condition of 0% of the demand not supplied should be a preferable choice for the PV-PHS hybrid system owner to reconstruct the original system. For other users without high requirements, all the solutions on the Pareto front can be used to design the system. A win-win solution on the Pareto front that is the results of overall trade-off between the two conflicting objectives should be provided to the planners. Such a solution does not only satisfy the users' demand for the reliability of power supply but also meet the investors' requirements on investment cost. The min-max fuzzy satisfying method is widely employed to find the best possible solution on the Pareto front. For the method, the result corresponding to the maximum weakest membership function is considered as the win-win solution. As shown in Table 4, the win-win solution is solution #8 where the maximum weakest membership function is 0.810287. The results of LCOE and PDNS under solution #8 are 0.0621 $/kWh and 0.7474%, respectively.

Due to the policy requirements, in some areas, the curtailment rate of renewable energy should be considered at

TABLE 4 Pareto optimal solutions obtained by MOPSO

#	LCOE, $/kWh	PDNS, %	ϕ_1, pu	ϕ_2, pu	min(ϕ_1, ϕ_2)
1	0.1834	0	0	1	0
2	0.1729	0.0260	0.070140	0.995167	0.070140
3	0.1563	0.0926	0.181029	0.982788	0.181029
4	0.1314	0.1083	0.347361	0.979870	0.347361
5	0.1222	0.1550	0.408818	0.971190	0.408818
6	0.0876	0.2862	0.639947	0.946803	0.639947
7	0.0687	0.5549	0.766199	0.896859	0.766199
8	0.0621	0.7474	0.810287	0.861078	0.810287
9	0.0559	1.1740	0.851703	0.781784	0.781784
10	0.0539	1.3650	0.865063	0.746283	0.746283
11	0.0518	1.5890	0.879092	0.704647	0.704647
12	0.0498	1.8850	0.892452	0.649628	0.649628
13	0.0478	2.2260	0.905812	0.586245	0.586245
14	0.0458	2.5890	0.919172	0.518773	0.518773
15	0.0438	2.9850	0.932532	0.445167	0.445167
16	0.0418	3.1060	0.945892	0.422677	0.422677
17	0.0398	3.8650	0.959252	0.281599	0.281599
18	0.0378	4.3330	0.972612	0.194610	0.194610
19	0.0357	4.8290	0.98664	0.102416	0.102416
20	0.0337	5.3800	1	0	0

Abbreviations: MOPSO, multiobjective particle swarm optimization; PDNS, percentage of the demand not supplied; LCOE, levelized cost of energy.

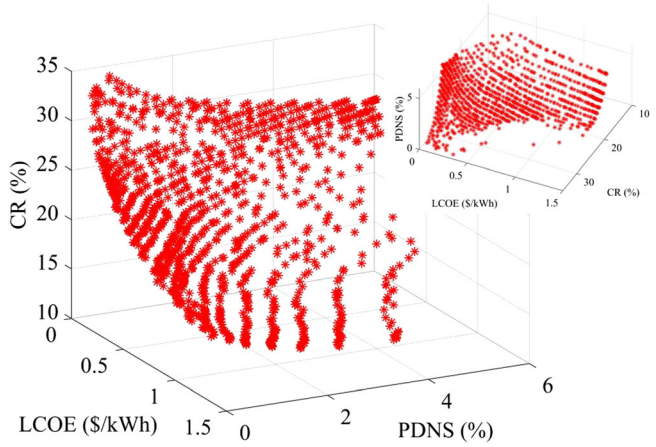

FIGURE 21 Triobjective optimization of the percentage of the demand not supplied (PDNS), levelized cost of energy (LCOE), and curtailment rate (CR) [Colour figure can be viewed at wileyonlinelibrary.com]

the stage of planning. Therefore, on the basis of biobjective, the curtailment rate of renewable energy as another objective function is introduced to form a triobjective optimization. Figure 21 presents the results of triobjective optimization of PDNS, LCOE, and CR. In order to clearly show the relationship between the three objectives, a small figure in the upper right corner of Figure 21 is given, which is seen from a different perspective. In Figure 21, it can be observed that the LCOE grows with the decrease of the CR under the same PDNS. Integrating wind turbines into the PV-PHS hybrid energy system will lead to the increase of CR; storage systems can be an effective way to reduce the CR. Considering the capacity of PHS cannot be adjusted in the research, only the battery can be used to reduce the CR. Due to the high investment cost of battery, the LCOE will increase significantly when the CR requirement is strict (low CR). The above analysis of biobjective (LCOE and PDNS) without considering CR can be applied to the condition considering CR. Likewise, under the same CR, the LCOE decreases with the increase of PDNS. Therefore, the requirements for CR and PDNS are big drawbacks for investors since the LCOE relates to CR and PDNS.

5 | CONCLUSION

This paper puts forward a novel concept of repowering an existing standalone hybrid energy system. A repowering strategy is proposed to reconstruct an existing PV-PHS hybrid energy system in Xiaojin, Sichuan, China, which is to integrate the battery bank and wind turbines into the existing PV-PHS hybrid energy system, in order to maximize the value of a PV-PHS hybrid system and fulfill the load demand in 5 years. Based on the actual requirements of PDSN and CR, the results can guide the planners to make the decision in Xiaojin, Sichuan, China. For the repowering strategy, the wind turbines can provide more power to the system and the battery bank as an auxiliary storage device of the PHS can help to implement the maximum reliability. A PMS is proposed and applied in simulations to manage the behaviors of the PHS and battery. The repowering strategy is optimized and investigated by means of the single-objective, biobjective, and triobjective PSO technique.

Simulation results of single-objective are analyzed in details, which is under zero PDNS and without considering CR. In this case, the battery plays an important role in ensuring zero PDNS. The comparative analysis of PSO and GA indicates that PSO performs better. During the biobjective optimization, the Pareto front set is found based on LCOE and PDNS. The LCOE can reduce by 81.6% if the acceptable PDNS varies from 0% to 5.38%. Thus, if a small PDNS is tolerated, significant reductions in LCOE can be reached. MOPSO is also compared with WSA, and they can obtain very similar Pareto font. In order to give the planners a win-win solution on the Pareto front, fuzzy satisfying method is utilized. Under the triobjective optimization, the CR is introduced due to the policy requirements. Repowering optimization is very significant for the existing PV-PHS hybrid system to meet the new requirements and policies. The results indicate that the requirements for CR and PDNS are unfavorable for the investors since the investment cost is greatly influenced by CR and PDNS. The theories and methods proposed in this paper can be applied in other hybrid systems, such as wind-PHS hybrid system and wind-battery hybrid system.

ACKNOWLEDGEMENT

This work was supported by the National Key Research and Development Program of China (2018YFB0905200).

NOMENCLATURE

C_{cap_bat}, C_{cap_wt} ($)	capital cost of the battery and wind turbines
C_{main_bat}, C_{main_wt} ($)	operation and maintenance cost of the battery and wind turbines
C_{rep_bat}, C_{rep_wt} ($)	replacement cost of the battery and wind turbines
C_{rep} ($)	replacement cost of each component
CRF	capital recovery factor

$E_{Bat}(t)$, $E_{Bat}(t-1)$ (kWh)	energy stored in the battery bank at hour t and t-1
$E_{Bat,max}$ (kWh)	maximum capacity of the battery bank
E_{Bat} (kWh)	energy stored in the battery
E_{served} (kWh)	energy supplied by the wind turbines and battery
e_{PV} (kW)	forecast error of PV output
e_{WT} (kW)	forecast error of wind turbines output
f (%)	annual inflation rate
G_T (W/m^2)	solar radiation
G_{ref} (W/m^2)	solar radiation at reference conditions, equal to 1000
g (m/s^2)	gravitational acceleration, equal to 9.81
H_{ref} (m)	reference height
H_{WT} (m)	installation height of the wind turbine
h (m)	height difference between upper and lower reservoir
$i/i^{'}$ (%)	nominal/Discount interest rate
k_P (1/°C)	temperature coefficient of peak power, equal to -3.7×10^{-3}
N_{PV}	the number of PV array in the original system
N_{rem} (year)	residual life of each device at the end of project lifetime
N_{life} (year)	lifetime of each component
P_R (kW)	rated power of PV module at reference conditions
P_{PV} (kW)	output power of the PV array
P_{PV}^{u} (kW)	forecast of PV power
P_{WTR} (W)	rated power of the wind turbines
P_{WTout} (kW)	output power of the wind turbines
P_{WTout}^{u} (kW)	forecast of wind power
P_w (kW)	output power of the water turbine
P_p (kW)	power supplied to the pump
P_{ch} (kW)	charged power of the battery bank
P_{dis} (kW)	discharged power of the battery bank
$P_{bat,max}$ (kW)	maximum charge/discharge power
$P_{load}(t)$ (kW)	load demand at hour t
P_w(t) (kW)	output power of the water turbine at hour t
$P_{dis}(t)$ (kW)	discharged power of the battery bank at hour t
$P_{PV}(t)$, $P_{WT}(t)$ (kW)	power directly supplied from PV array and wind turbines at hour t
PDNS, PDNS1 (%)	percentage of the demand not supplied of the original system and repowering strategy
q_w (m^3/s)	water flow rate input into the water turbine
q_p (m^3/s)	water flow rate output from the pump
$Q_{UR}(t)$, $Q_{UR}(t-1)$ (m^3)	water quantity of the upper reservoir at hour t and t-1
$Q_{UR,min}$, $Q_{UR,max}$ (m^3)	lower and upper limits of the upper reservoir
Q_{UR} (m^3)	the water quantity stored in the upper reservoir
SOC_{min},SOC_{max} (%)	the bottom and top limitation of battery state of charge
SV ($)	salvage value
T_C (°C)	PV module temperature
T_{ref} (°C)	PV module temperature at reference conditions, equal to 25
T_{amb} (°C)	ambient temperature
V_R (m/s)	rated wind speed at which the wind turbine reaches its rated power
V_{ref} (m/s)	wind speed at the reference height
V_{ci}, V_{co} (m/s)	the cut-in and cut-out wind speeds, the speeds where the wind turbine begins to generate electricity or shut down
V (m/s)	wind speed at the installation height of the wind turbine
V_{UR} (m^3)	capacity of the upper reservoir
x	binary decision variable
y (year)	lifetime of the project
β	water loss coefficient which is similar to self-discharge coefficient
η_{PV} (%)	the efficiency of the inverter
η_w (%)	overall efficiency of the water turbine
η_p (%)	overall efficiency of the pump
η_{ch},η_{dis} (%)	charge and discharge efficiency of the battery bank
λ	power law coefficient which is related to the selected location

ρ (kg/m^3)	water density, equal to 1
ϕ_i^n	membership function for the nth solution of ith objective function
$\phi_i^{\max}/\phi_i^{\min}$	maximum/minimum value of ith objective function
ϕ^n	membership function of nth solution
$\phi^{\max}$	maximum weakest membership function

ORCID

Xiao Xu https://orcid.org/0000-0002-3714-4943

REFERENCES

1. China Industry Information, Analysis on the development status and development trend of global new energy power generation in 2017, http://www.chyxx.com/industry/201801/600024.html [accessed 21 July 2018].
2. Balali MH, Nouri N, Rashidi M, Nasiri A, Otieno W. A multi-predictor model to estimate solar and wind energy generations. *International Journal of Energy Research*. 2018;42(2):696-706.
3. Ming T, Meng F, Liu W, Pan Y, Kiesgen de Richter R. Analysis of output power smoothing method of the solar chimney power generating system. *International Journal of Energy Research*. 2013;37(13):1657-1668.
4. Eser P, Chokani N, Abhari RS. Impacts of battery electric vehicles on renewable integration within the 2030 European power system. *International Journal of Energy Research*. 2018;42(13):4142-4156.
5. Baghdadi F, Mohammedi K, Diaf S, Behar O. Feasibility study and energy conversion analysis of stand-alone hybrid renewable energy system. *Energy Conversion and Management*. 2015;105:471-479.
6. Awan AB, Zubair M, Sidhu GAS, Bhatti AR, Abo-Khalil AG. Performance analysis of various hybrid renewable energy systems using battery, hydrogen, and pumped hydro-based storage units. *International Journal of Energy Research*. 2018;1-26.
7. Balali MH, Nouri N, Omrani E, Nasiri A, Otieno W. An overview of the environmental, economic, and material developments of the solar and wind sources coupled with the energy storage systems. *International Journal of Energy Research*. 2017;41(14):1948-1962.
8. Acar C. A comprehensive evaluation of energy storage options for better sustainability. *International Journal of Energy Research*. 2018;42(12):3732-3746.
9. Zhang QL, Wu HG. Embedment of steel spiral cases in concrete: China's experience. *Renewable and Sustainable Energy Reviews*. 2017;72:1271-1281.
10. Al-Shamma'a AA, Addoweesh KE. Techno-economic optimization of hybrid power system using genetic algorithm. *International Journal of Energy Research*. 2017;38:1608-1623.
11. Sharafi M, ElMekkawy TY. A dynamic MOPSO algorithm for multiobjective optimal design of hybrid renewable energy systems. *International Journal of Energy Research*. 2014;38(15):1949-1963.
12. Sanajaoba S, Fernandez E. Maiden application of Cuckoo search algorithm for optimal sizing of a remote hybrid renewable energy system. *Renewable Energy*. 2016;96(A):1-10.
13. Shi Z, Wang R, Zhang T. Multi-objective optimal design of hybrid renewable energy systems using preference-inspired coevolutionary approach. *Solar Energy*. 2015;118:96-106.
14. Bahramara S, Parsa Moghaddam M, Haghifam MR. Optimal planning of hybrid renewable energy systems using HOMER: A review. *Renewable and Sustainable Energy Reviews*. 2016;62:609-620.
15. Nojavan S, Majidi M, Najafi-Ghalelou A, Ghahramani M, Zare K. A cost-emission model for fuel cell/PV/battery hybrid energy system in the presence of demand response program: ε-constraint method and fuzzy satisfying approach. *Energy Conversion and Management*. 2017;138:383-392.
16. Majidi M, Nojavan S, Esfetanaj NN, Najafi-Ghalelou A, Zare K. A multi-objective model for optimal operation of a battery/PV/fuel cell/grid hybrid energy system using weighted sum technique and fuzzy satisfying approach considering responsible load management. *Solar Energy*. 2017;144:79-89.
17. Hou J, Xu P, Lu X, Pang Z, Chu Y, Huang G. Implementation of expansion planning in existing district energy system: a case study in China. *Applied Energy*. 2018;211:269-281.
18. Candas S, Siala K, Hamacher T. Sociodynamic modeling of small-scale PV adoption and insights on future expansion without feed-in tariffs. *Energy Policy*. 2019;125:521-536.
19. ZekiYılmazoğlu M, Durmaz A, Baker D. Solar repowering of Soma—a thermal power plant. *Energy Conversion and Management*. 2012;64:232-237.
20. Serri L, Lembo E, Airoldi D, Gelli C, Beccarello M. Wind energy plants repowering potential in Italy: technical-economic assessment. *Renewable Energy*. 2018;115:382-390.
21. Hou P, Enevoldsen P, Hu W, Chen C, Chen Z. Offshore wind farm repowering optimization. *Applied Energy*. 2017;208:834-844.
22. Lan H, Wen S, Hong YY, David CY, Zhang L. Optimal sizing of hybrid PV/diesel/battery in ship power system. *Applied Energy*. 2015;158:26-34.
23. Bortolini M, Gamberi M, Graziani A, Pilati F. Economic and environmental bi-objective design of an off-grid photovoltaic–battery–diesel generator hybrid energy system. *Energy Conversion and Management*. 2015;106:1024-1038.
24. Gökçek M, Kale C. Techno-economical evaluation of a hydrogen refuelling station powered by Wind-PV hybrid power system: a case study for İzmir-Çeşme. *International Journal of Hydrogen Energy*. 2018;43(23):10615-10625.
25. Daud AK, Ismail MS. Design of isolated hybrid systems minimizing costs and pollutant emissions. *Renewable Energy*. 2012;44:215-224.
26. Azaza M, Wallin F. Multi objective particle swarm optimization of hybrid micro-grid system: a case study in Sweden. *Energy*. 2017;123:108-118.

27. Yang H, Zhou W, Lu L, Fang Z. Optimal sizing method for stand-alone hybrid solar–wind system with LPSP technology by using genetic algorithm. *Solar Energy*. 2008;82(4):354-367.
28. Kusakana K. Optimization of the daily operation of a hydrokinetic–diesel hybrid system with pumped hydro storage. *Energy Conversion and Management*. 2015;106:901-910.
29. Bortolini M, Gamberi M, Graziani A. Technical and economic design of photovoltaic and battery energy storage system. *Energy Conversion and Management*. 2014;86:81-92.
30. Shin Y, Yong Koo W, Hyung Kim T, Jung S, Kim H. Capacity design and operation planning of a hybrid PV-wind-battery-diesel power generation system in the case of Deokjeok Island. *Applied Thermal Engineering*. 2015;89:514-525.
31. Maleki A, Pourfayaz F, Rosen MA. A novel framework for optimal design of hybrid renewable energy-based autonomous energy systems: a case study for Namin. *Iran. Energy*. 2016;98:168-180.
32. Huang Y, Keatley P, Chen HS, Zhang XJ, Rolfe A, Hewitt NJ. Techno-economic study of compressed air energy storage systems for the grid integration of wind power. *International Journal of Energy Research*. 2018;42(2):559-569.
33. Akinyele D. Analysis of photovoltaic mini-grid systems for remote locations: a techno-economic approach. *International Journal of Energy Research*. 2018;42(3):1363-1380.
34. https://www.homerenergy.com/pdf/HOMERHelpManual.pdf [Accessed 1 April 2019].
35. Majidi M, Nojavan S, Zare K. Optimal stochastic short-term thermal and electrical operation of fuel cell/photovoltaic/battery/grid hybrid energy system in the presence of demand response program. *Energy Conversion and Management*. 2017;144:132-142.
36. Ding H, Hu Z, Song Y. Stochastic optimization of the daily operation of wind farm and pumped-hydro-storage plant. *Renewable Energy*. 2012;48:571-578.
37. Shi Y, Eberhart RC. Empirical study of particle swarm optimization. *Proc Congr Evol Comput*. 1999;1950-1955.
38. Abido MA. Multiobjective particle swarm optimization for environmental/economic dispatch problem. *Electric Power Systems Research*. 2009;79(7):1105-1113.
39. Niknam T, Narimani MR, Aghaei J, Azizipanah-Abarghooee R. Improved particle swarm optimisation for multi-objective optimal power flow considering the cost, loss, emission and voltage stability index, *IET Generation. Transmission & Distribution*. 2012;6(6):515-527.
40. Castillo A, Gayme DF. Grid-scale energy storage applications in renewable energy integration: a survey. *Energy Conversion and Management*. 2014;87:885-894.
41. Hossain M, Mekhilef S, Olatomiwa L. Performance evaluation of a stand-alone PV-wind-diesel-battery hybrid system feasible for a large resort center in South China Sea, Malaysia. *Sustainable Cities and Society*. 2017;28:358-366.

How to cite this article: Xu X, Hu W, Cao D, Liu W, Chen Z, Lund H. Implementation of repowering optimization for an existing photovoltaic-pumped hydro storage hybrid system: A case study in Sichuan, China. *Int J Energy Res*. 2019;43:8463–8480. https://doi.org/10.1002/er.4846